Supporting Information

Multicolor polymeric carbon dots: synthesis, separation and polyamide-supported molecular fluorescence

Bo Zhi,[1,2†] Xiaoxiao Yao,[1†] Meng Wu,[3] Arielle Mensch,[4] Yi Cui,[4,5] Jiahua Deng,[6] Juan J Duchimaza-Heredia,[6] Kasidet Jing Trerayapiwat,[6] Thomas Niehaus,[7] Yoshio Nishimoto,[8] Benjamin P. Frank,[9] Yongqian Zhang,[10] Riley E. Lewis,[1] Elaine A. Kappel,[1] Robert J. Hamers,[10] Howard D. Fairbrother,[9] Galya Orr,[4] Catherine J. Murphy,[3] Qiang Cui,[6,11] and Christy L. Haynes[1*]

1 Department of Chemistry, University of Minnesota-Twin Cities, 207 Pleasant Street SE, Minneapolis, Minnesota 55455, United States

2 Current address: Advanced Performance Material Lab, Research and Development Center, ZEON Corporation, Kanagawa 210-9507, Japan

3 Department of Chemistry, University of Illinois at Urbana-Champaign, 600 South Mathews Avenue, Urbana, Illinois 61801, United States

4 Environmental Molecular Sciences Laboratory, Pacific Northwest National Laboratory, 3335 Innovation Boulevard, Richland, Washington 99352, United States

5 Current address: MIT Media Lab, Cambridge, MA 02139, United States

6 Department of Chemistry, Boston University, 590 Commonwealth Avenue, Boston, Massachusetts 02215, United States

7 Univ Lyon, Université Claude Bernard Lyon 1, CNRS, Institut Lumière Matière, F-69622 Lyon, France

8 Graduate School of Science, Kyoto University, Kyoto 606-8502, Japan

9 Department of Chemistry, Johns Hopkins University, Baltimore, MD 21218, United States

10 Department of Chemistry, University of Wisconsin-Madison, 1101 University Avenue, Madison, Wisconsin 53706, United States

11 Departments of Physics and Biomedical Engineering, Boston University, 590 Commonwealth Avenue, Boston, Massachusetts 02215, United States

† These two authors contributed equally to this work

*Corresponding author: chaynes@umn.edu

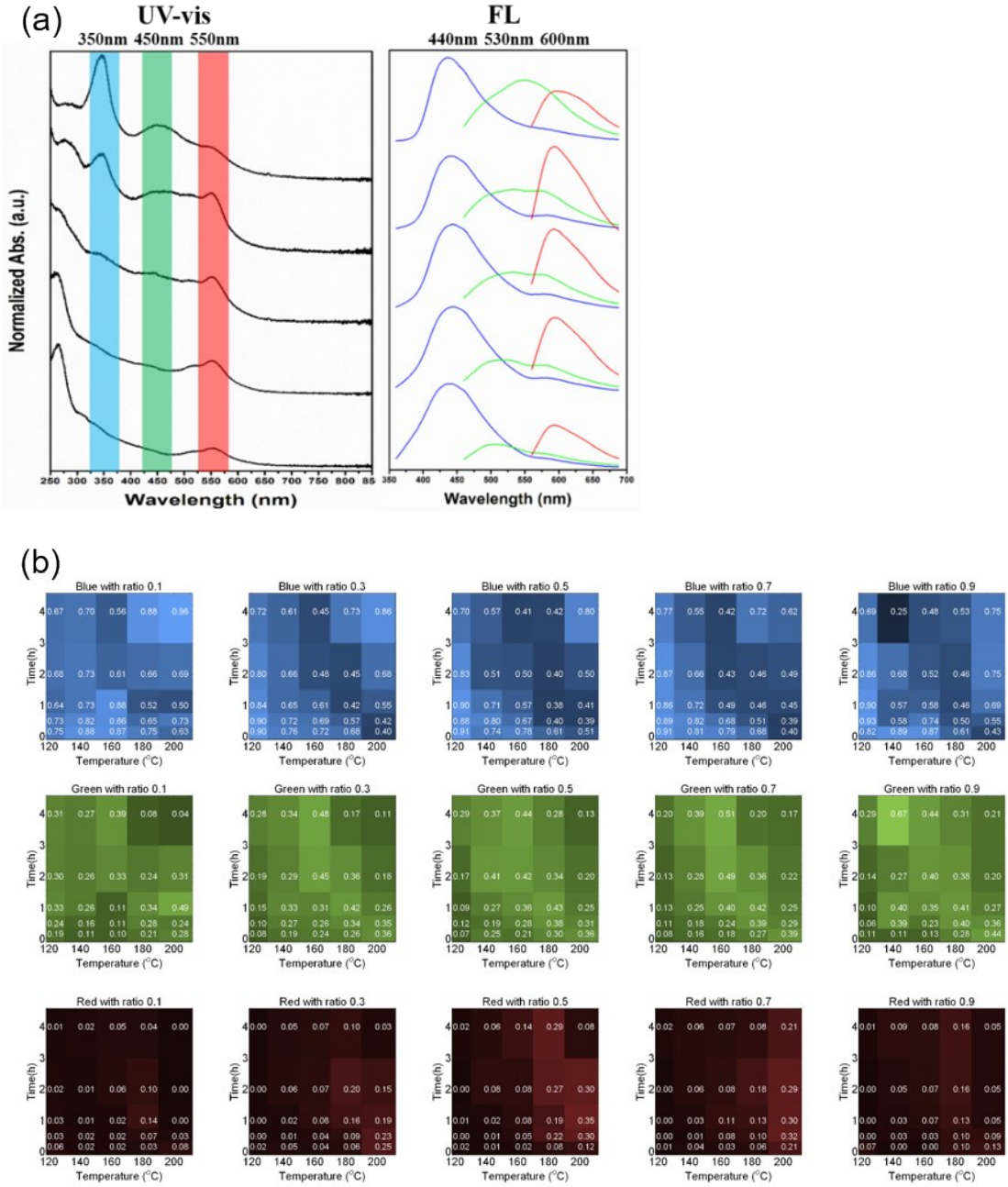

Figure S1. (a) A representative UV-vis (left) and fluorescence(right) spectra in the optimization of multicolor CDs synthesis. Peaks in the fluorescence spectra were integrated. (b) a summary chart showing the percentage of the integrated peak area in the blue, green, and red region of the raw products synthesized in the screening process. Citric acid to urea molar ratio was varied as 0.1, 0.3, 0.5, 0.7, and 0.9. Reaction temperature was 120 °C, 140 °C, 160 °C, 180 °C, and 200 °C. Reaction time was held to be 10 min, 30 min, 1 h, 2 h, and 4 h.

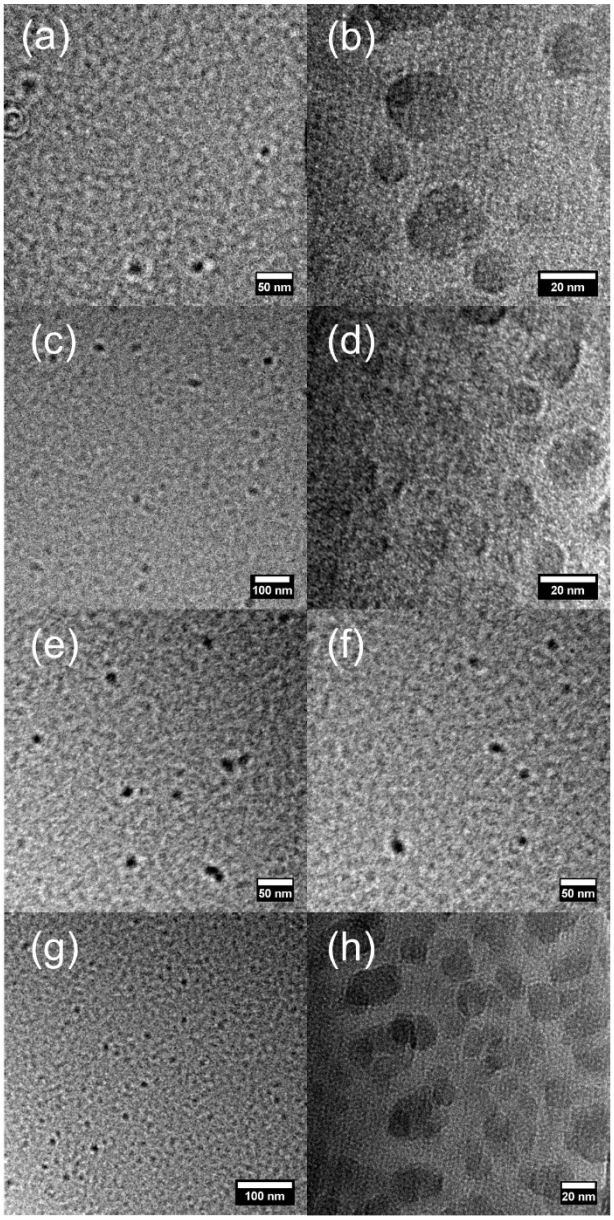

Figure S2. TEM images of (a)(b) as-made CDs; (c)(d) CD-B; (e)(f) CD-G; and (g)(h) CD-R.

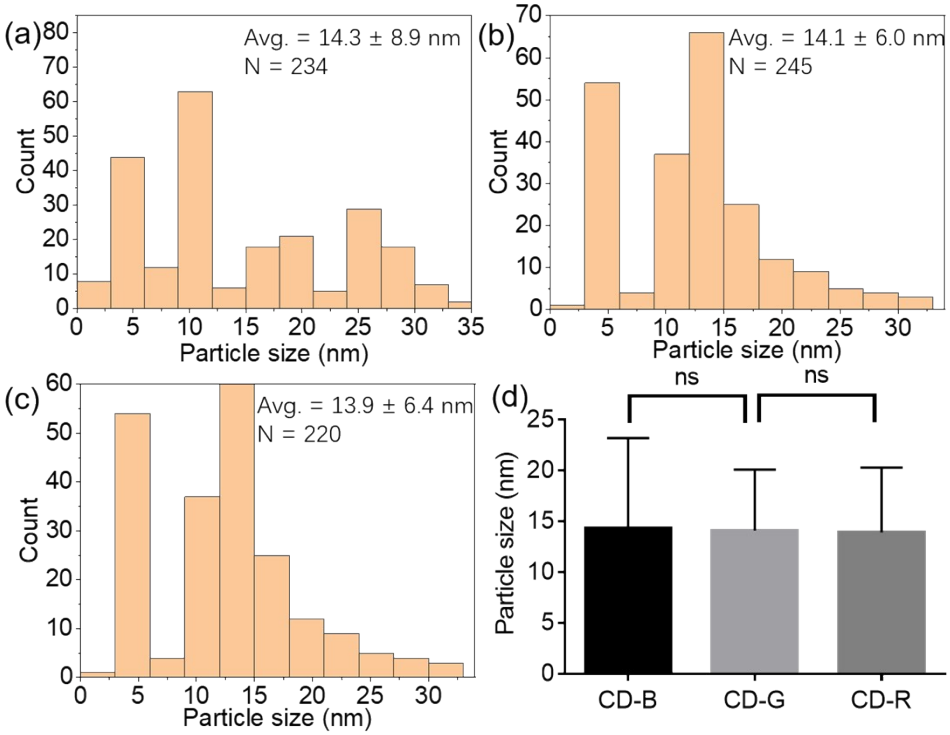

Figure S3. Histograms of particle sizes of (a) CD-B, (b) CD-G, and (c) CD-R, analyzed with ImageJ of TEM images. (d) One-way ANOVA analysis shows no statistical difference among CD-B, CD-G, and CD-R.

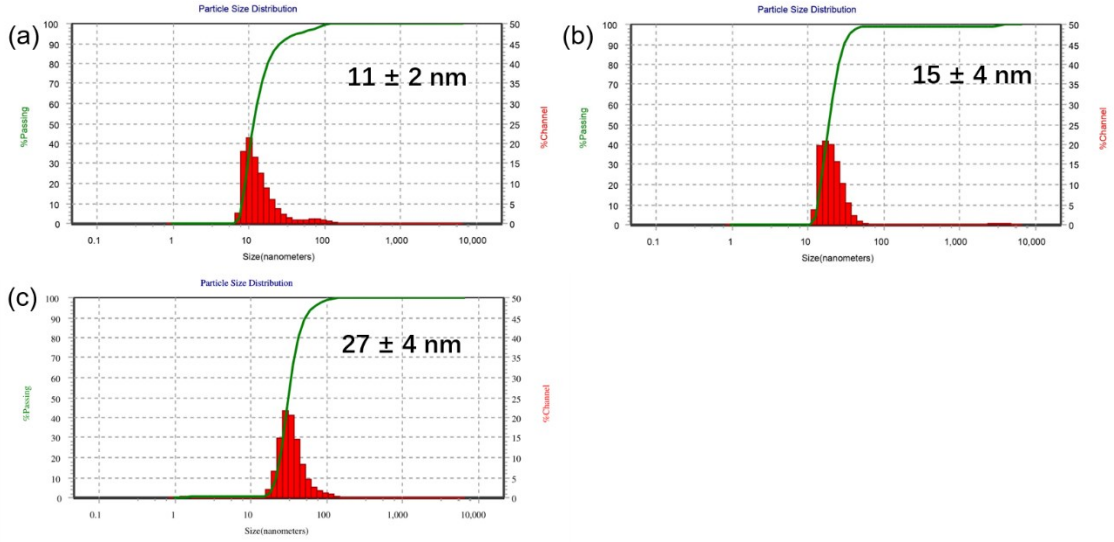

Figure S4. Dynamic light scattering (DLS) results of (a) CD-B, (b) CD-G, and (c) CD-R in deionized water.

The DLS sizes for CD-B, G, and R fractions are 11 ± 2 nm, 15 ± 4 nm, and 27 ± 4 nm, respectively. These CDs tended to form aggregates, which explains the slightly higher diameter of CD-R.

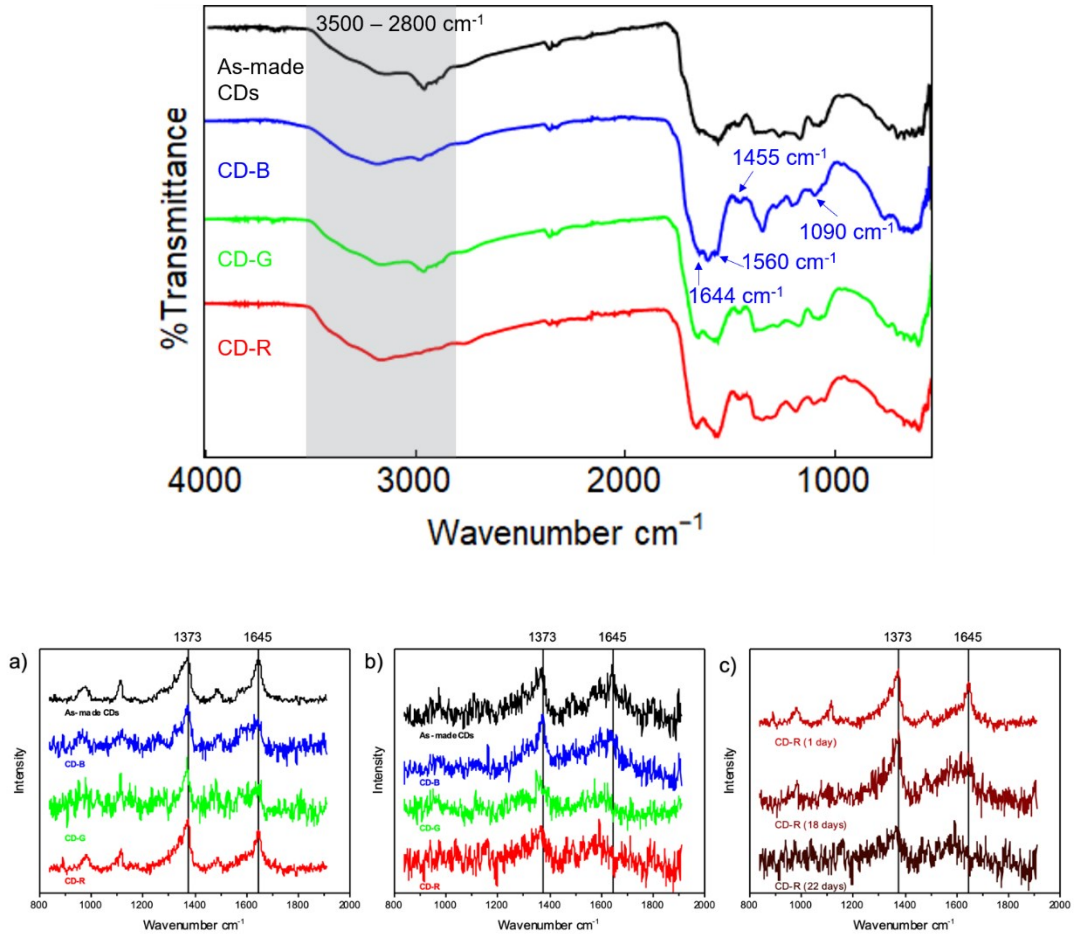

Figure S5. Raman spectra of as-made CDs and CD-B, CD-G, and CD-R (a) the day after synthesis and (b) 22 days after synthesis. (c) Raman spectra of CD-R at different time points after synthesis.

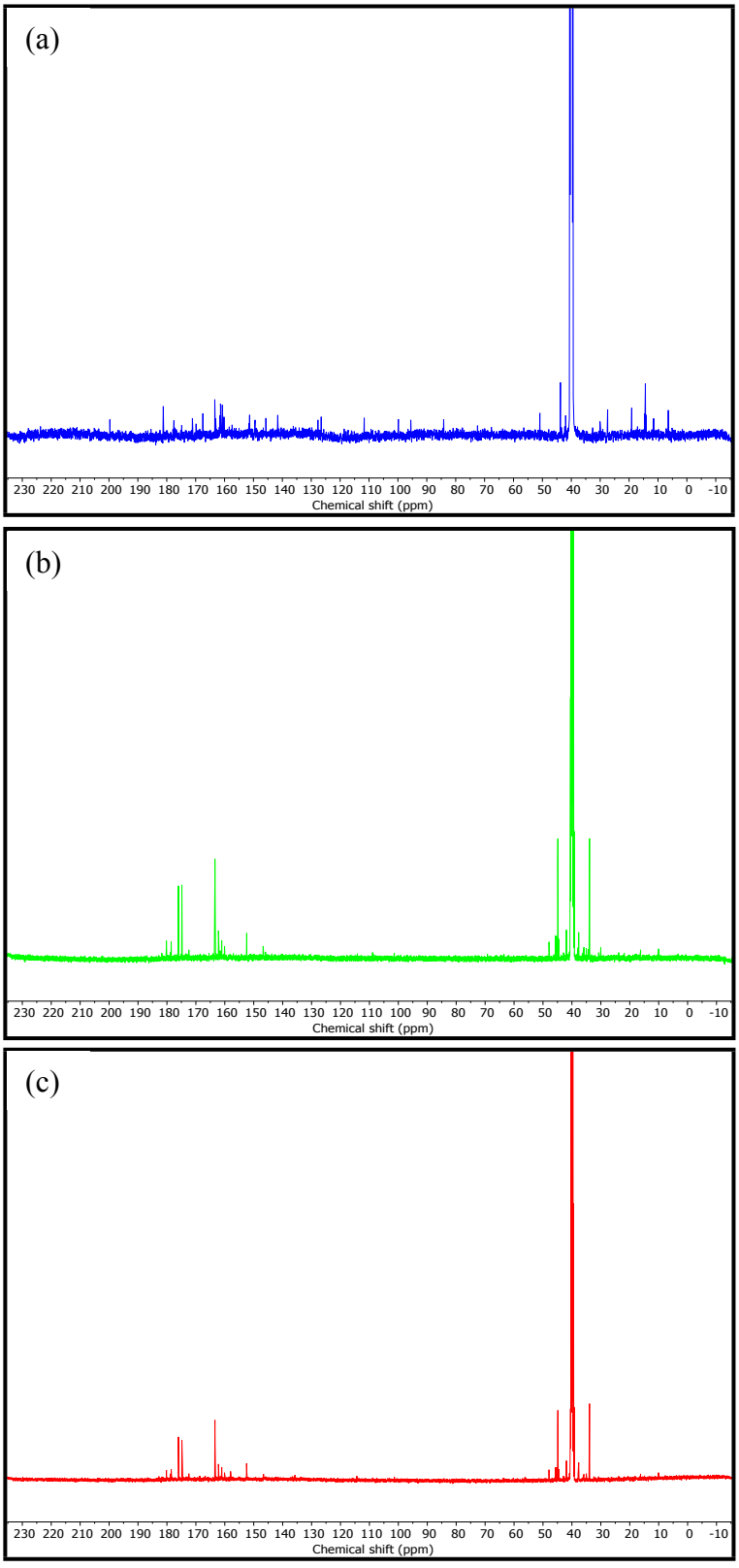

Figure S6. ^{13}C NMR spectra of CA-B (a), CA-G (b) and CA-R (c) before dialysis in DMSO-d_6. The strong peak at 40 ppm is the solvent peak. The peaks from 0-25 ppm correspond to C in methyl and -CH_2R groups. The peaks from 25-55 ppm correspond to C in C-N and -CHR_2 groups. The peaks from 50-90 ppm correspond to C in C-O groups. The peaks from 80-150 ppm correspond to C in C=C groups. The peaks beyond 150 ppm correspond to C in C=O groups.

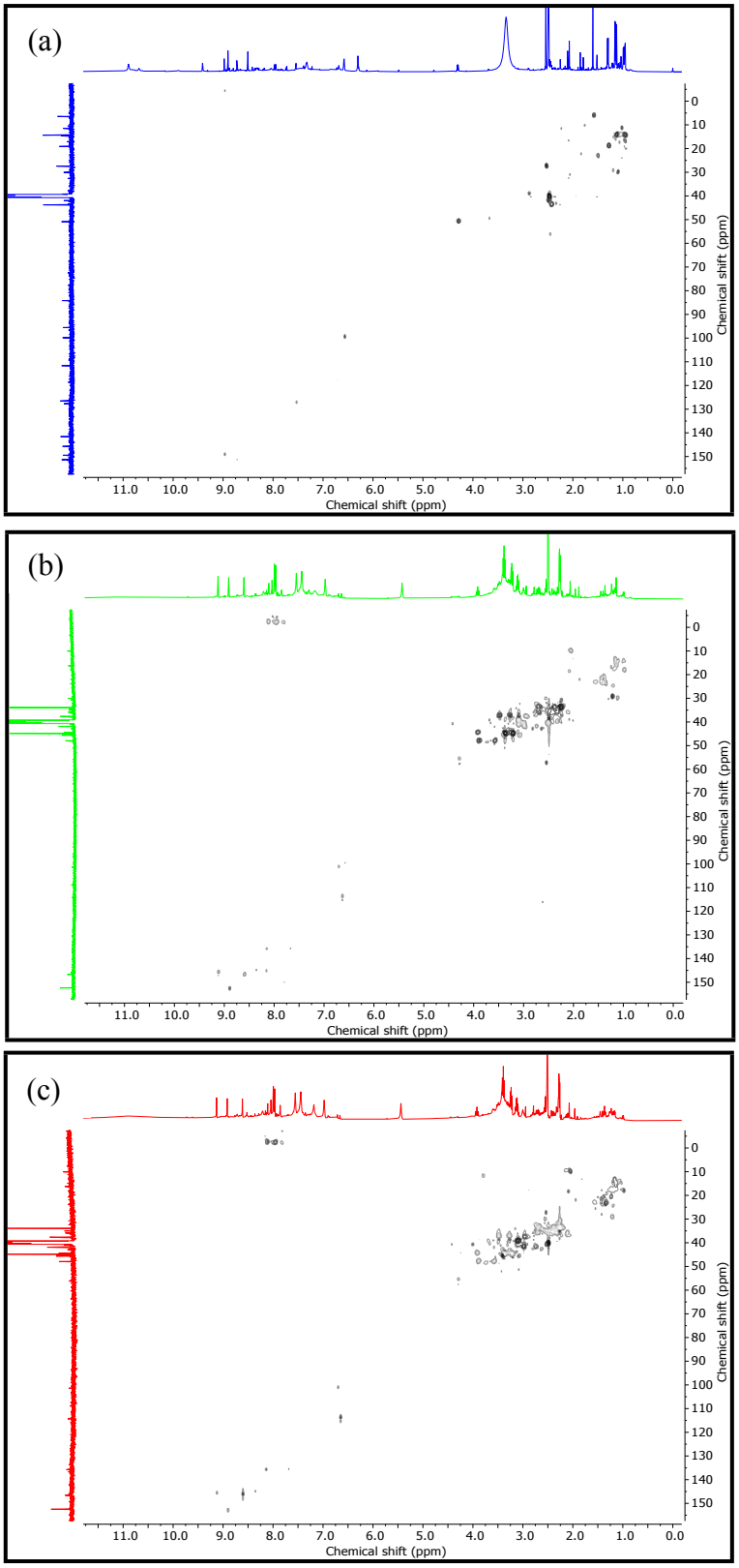

Figure S7. ^{1}H-^{13}C HSQC spectra of CA-B (a), CA-G (b) and CA-R (c) before dialysis in DMSO-d_6.

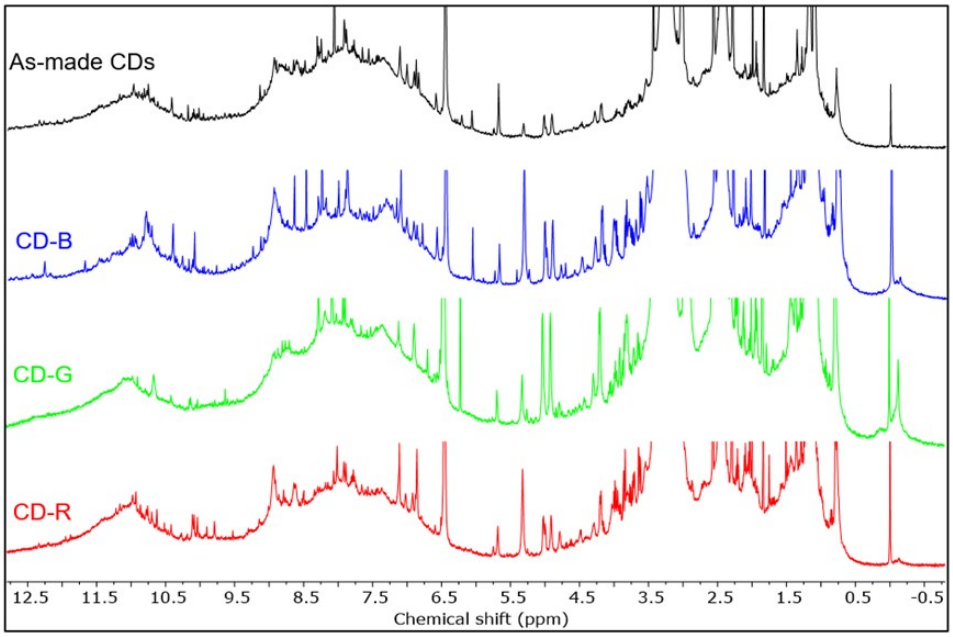

Figure S8. ^{1}H NMR spectra of as made CDs, CD-B, CD-G, and CD-R in DMSO-d6 after dialysis (magnified from Figure 4(b)).

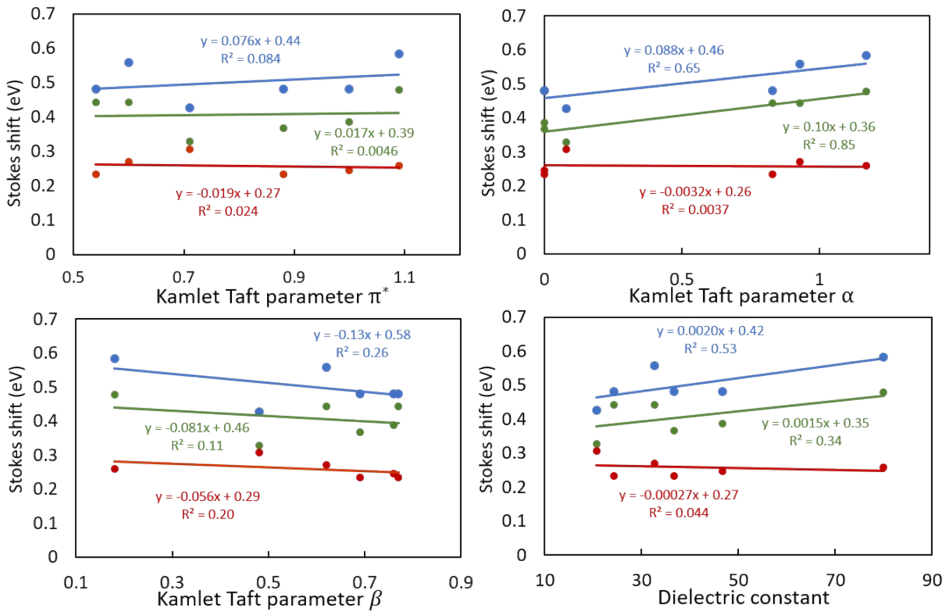

Figure S9. Stokes shift of CDs dispersed in acetone, DMF, DMSO, ethanol, methanol, and water against Kamlet Taft parameters π^*, α, and β and dielectric constant.

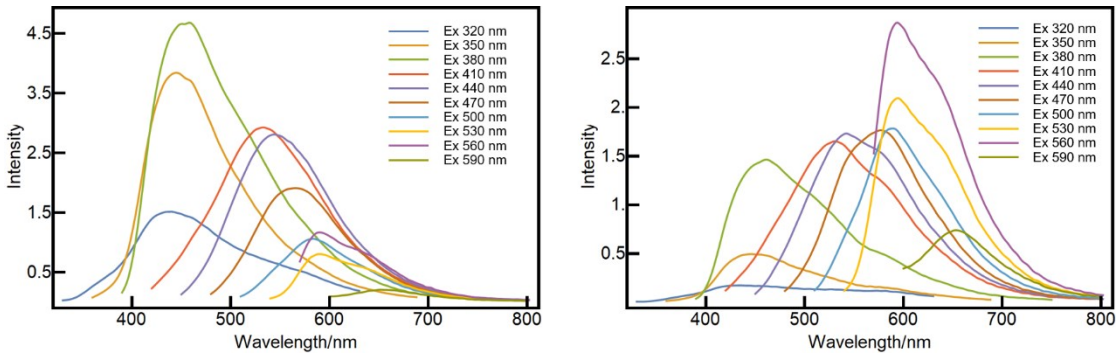

Figure S10. Fluorescence spectra of dialysate separated from filtered raw product through membrane 100-500 Da (left) and 3500 Da (right).

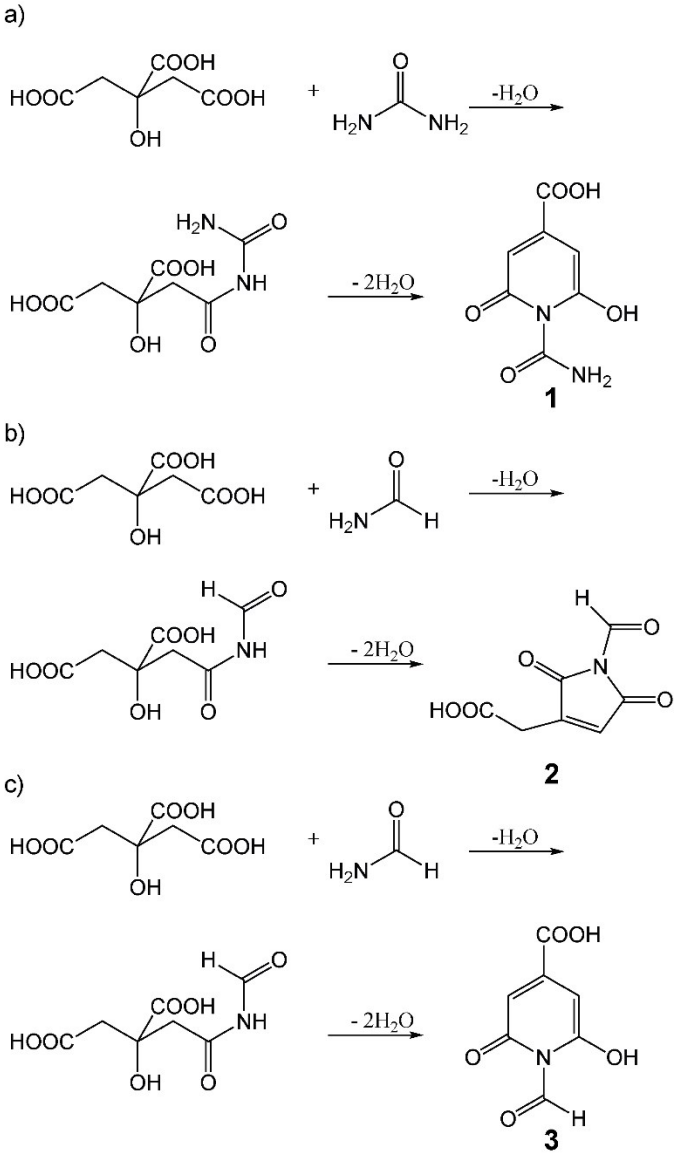

Figure S11. Proposed reaction pathways that lead to the formation of small molecule chromophores starting with citric acid, urea and formamide.

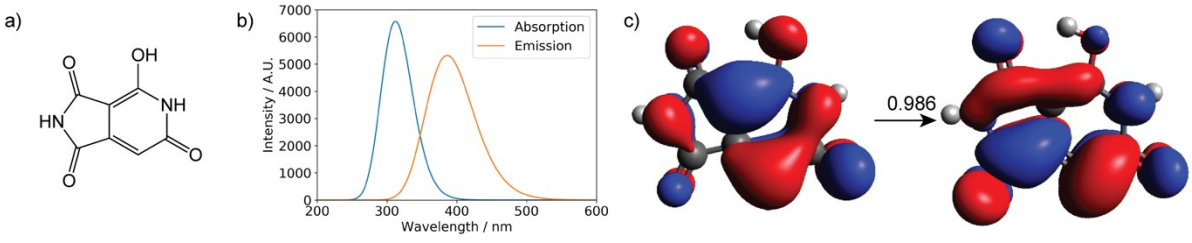

Figure S12. (a) Chemical structures, (b) calculated UV-Vis absorption, fluorescence spectra, and (c) natural transition orbitals of 4-hydroxy-1H-pyrrolo[3,4-c]pyridine-1,3,6(2H,5H)-trione (HPPT).

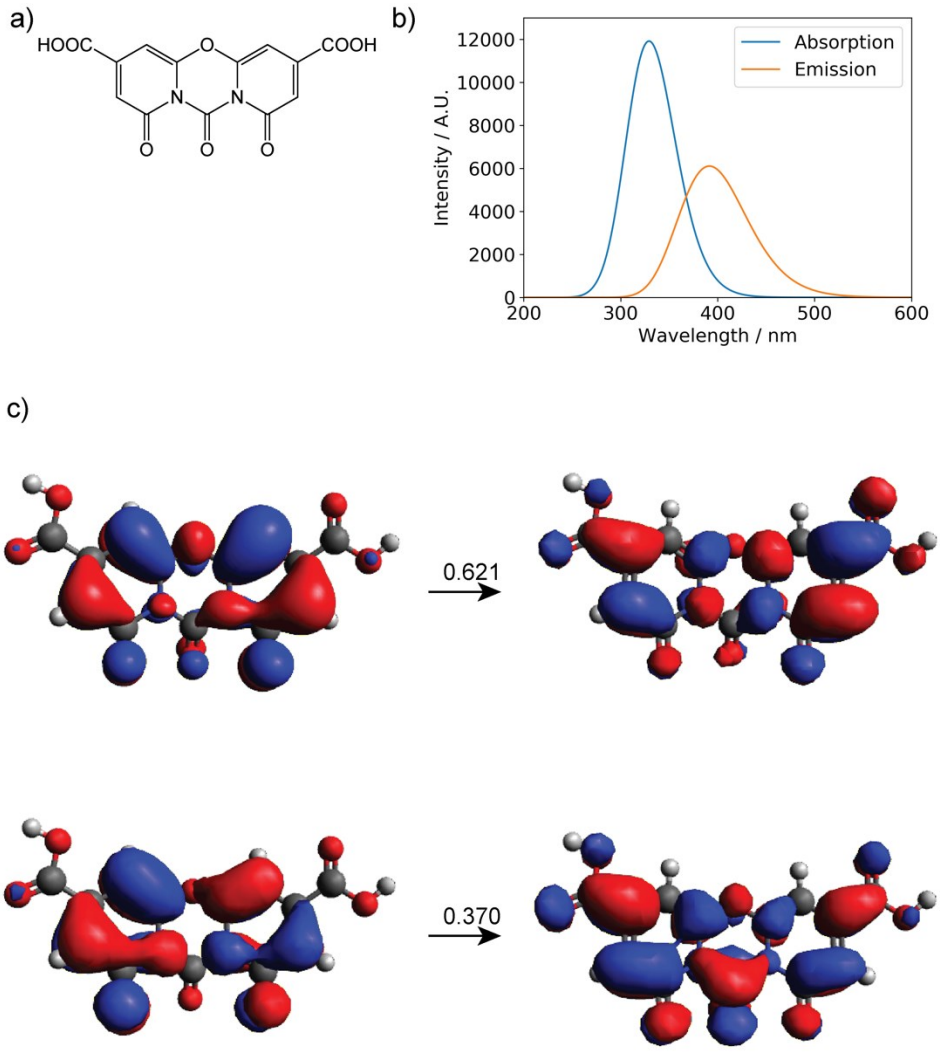

Figure S13. (a) Chemical structures, (b) calculated UV-Vis absorption, fluorescence spectra, and (c) natural transition orbitals of a small molecule chromophore formed from further condensation of molecule **3** in Figure S10.

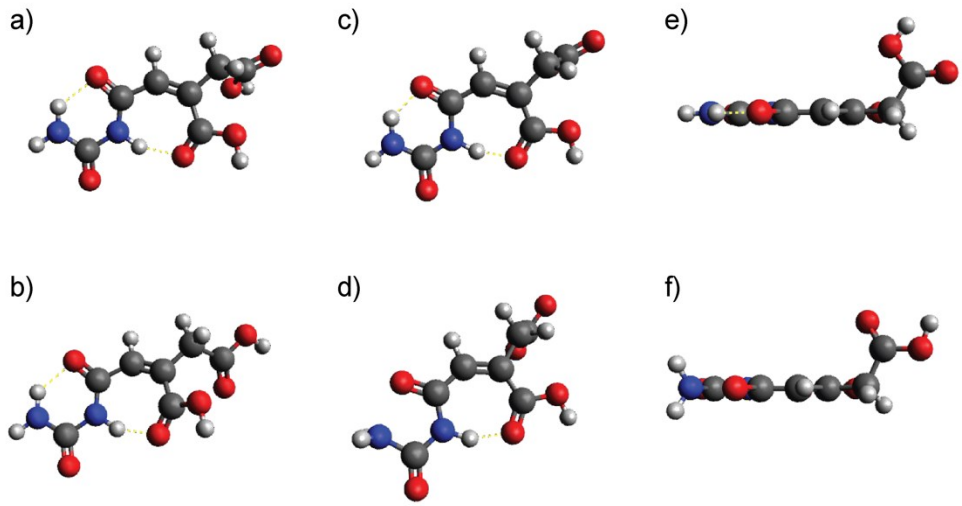

Figure S14. Optimized structures of the dehydrated amide monomer. (a-b) Optimized structures of the ground state, (c-d) optimized structures of the first excited state, and (e-f) the side view of the first excited state. The first row shows results at the level of B3LYP/6-31+G(d,p), and the second row shows results at the level of ωB97XD/6-31+G(d,p). In the first excited state minimum, the orientation of the NH_2 group is different at the two levels of theory, and exchanging the initial structure for optimization does not change the result. As shown in Table S15, both conformers are local minima at the CAM-B3LYP level of theory.

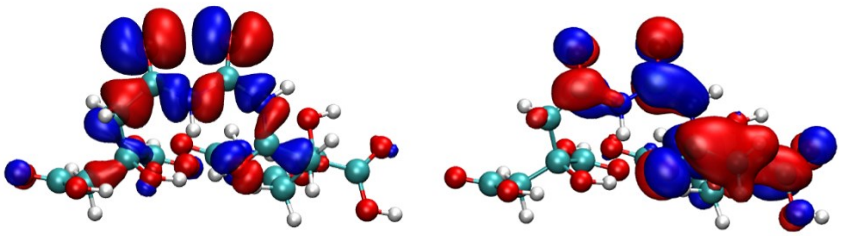

Figure S15. Orbitals with the leading transition coefficient (HOMO and LUMO) for the S0→S1 excitation of the polyamide dimer of citric acid and urea (ID0) calculated with LC-TD-DFTB2. The leading excitation is n→π* in nature. The HOMO/LUMO calculated with ωB97XD are visually equivalent.

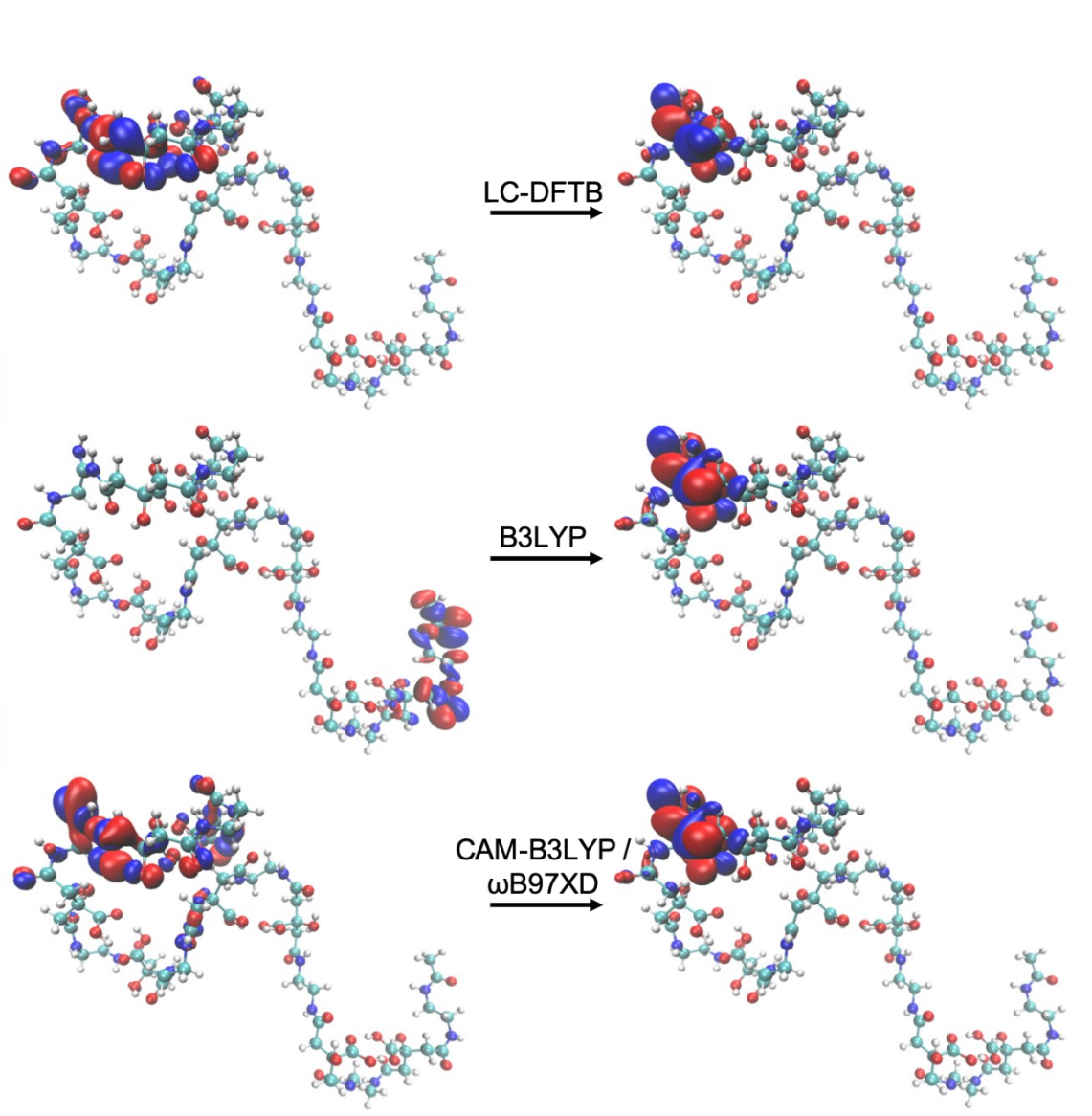

Figure. S16. The HOMO and LUMO orbitals for the polyamide (octamer) formed between citric acid and ethylene diamine studied in Ref. 1. Clearly, the S1 excitation at the B3LYP level is charge transfer in nature, while the nature of excitation is local when range-separation functionals are used in either TD-DFT or TD-DFTB calculations.

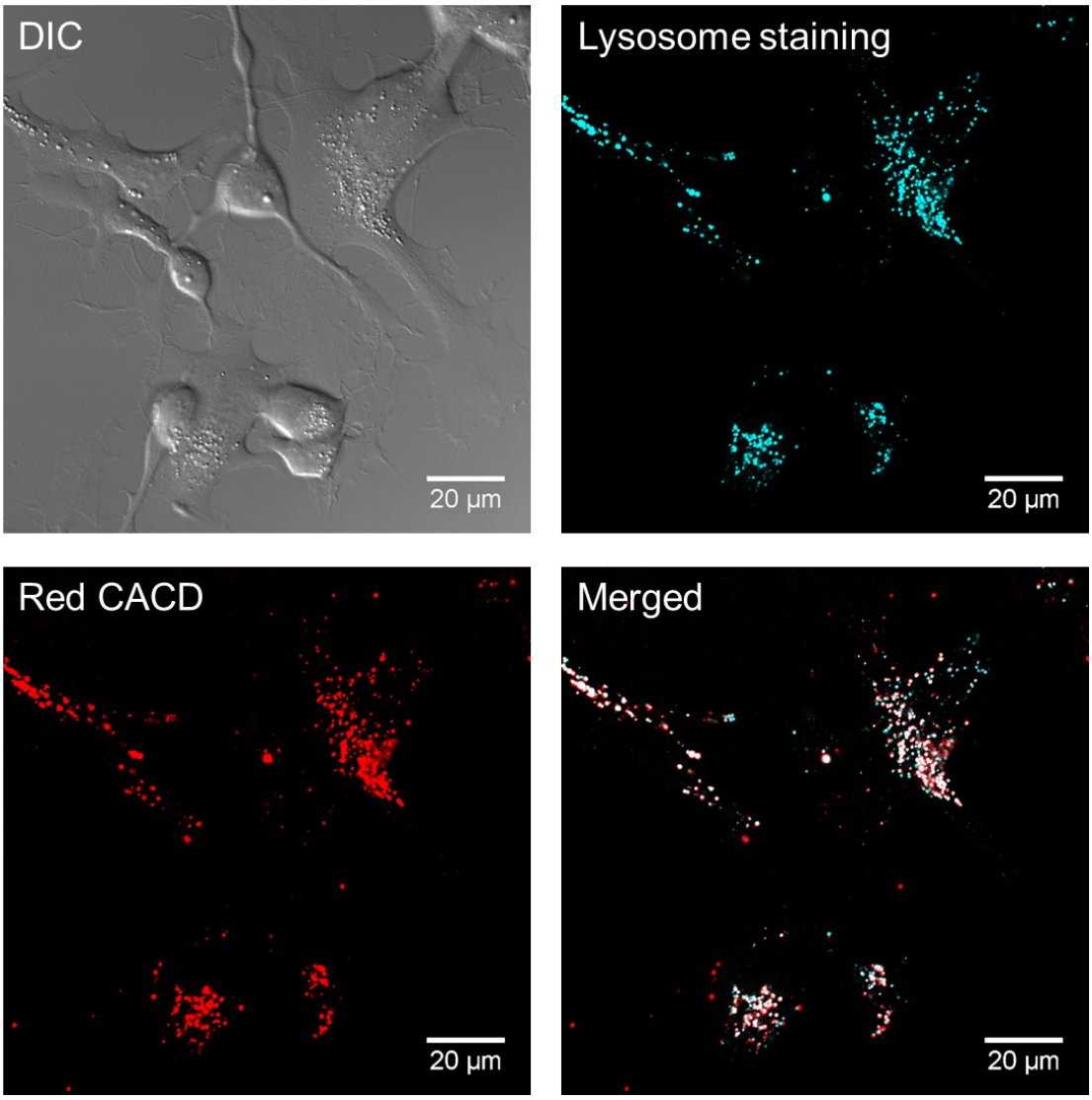

Figure S17. Red CDs mainly localizes in lysosomes upon uptake into trout gill epithelial cells.

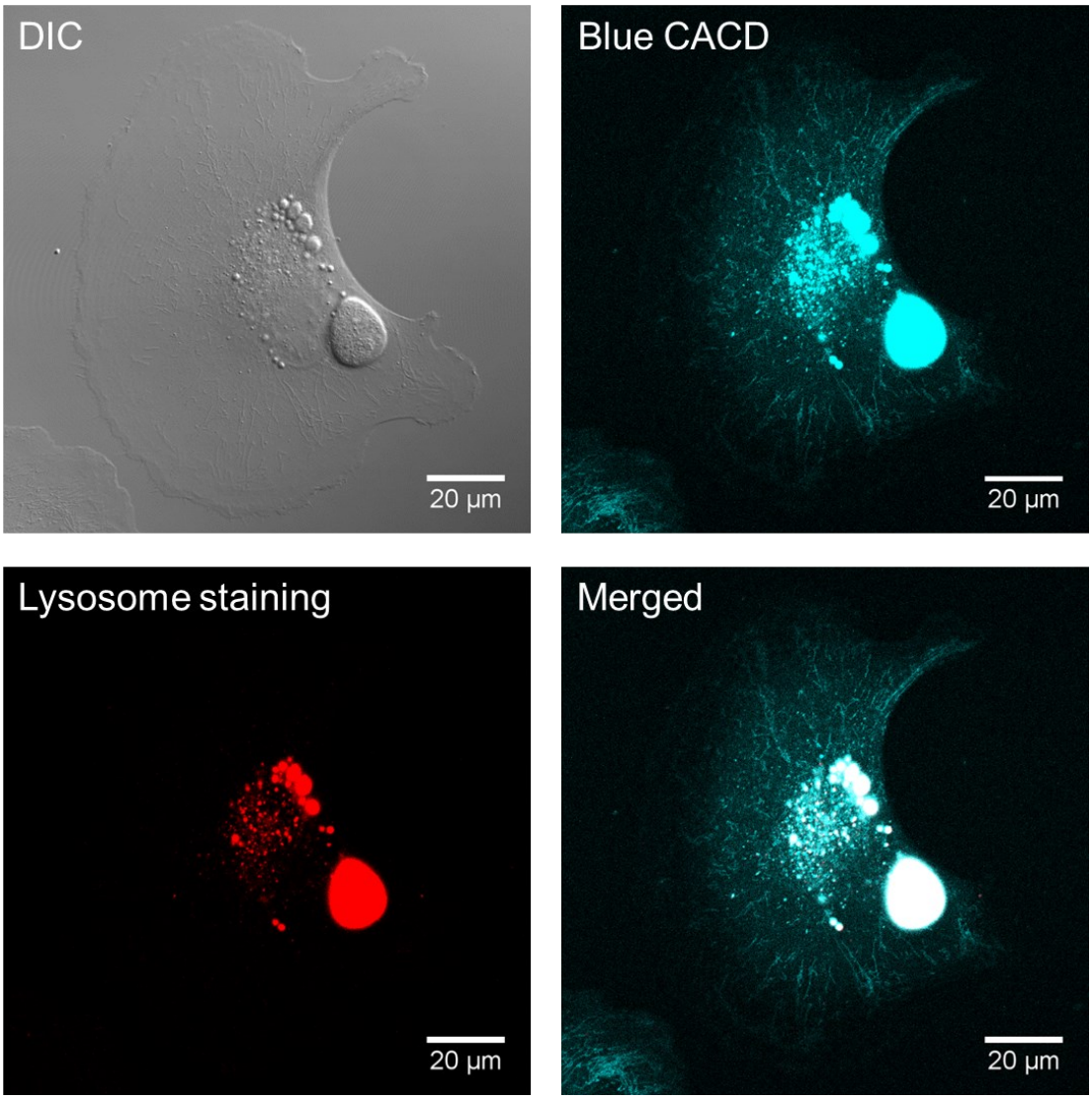

Figure S18. Some blue CDs localize in lysosomes upon uptake into trout gill epithelial cells.

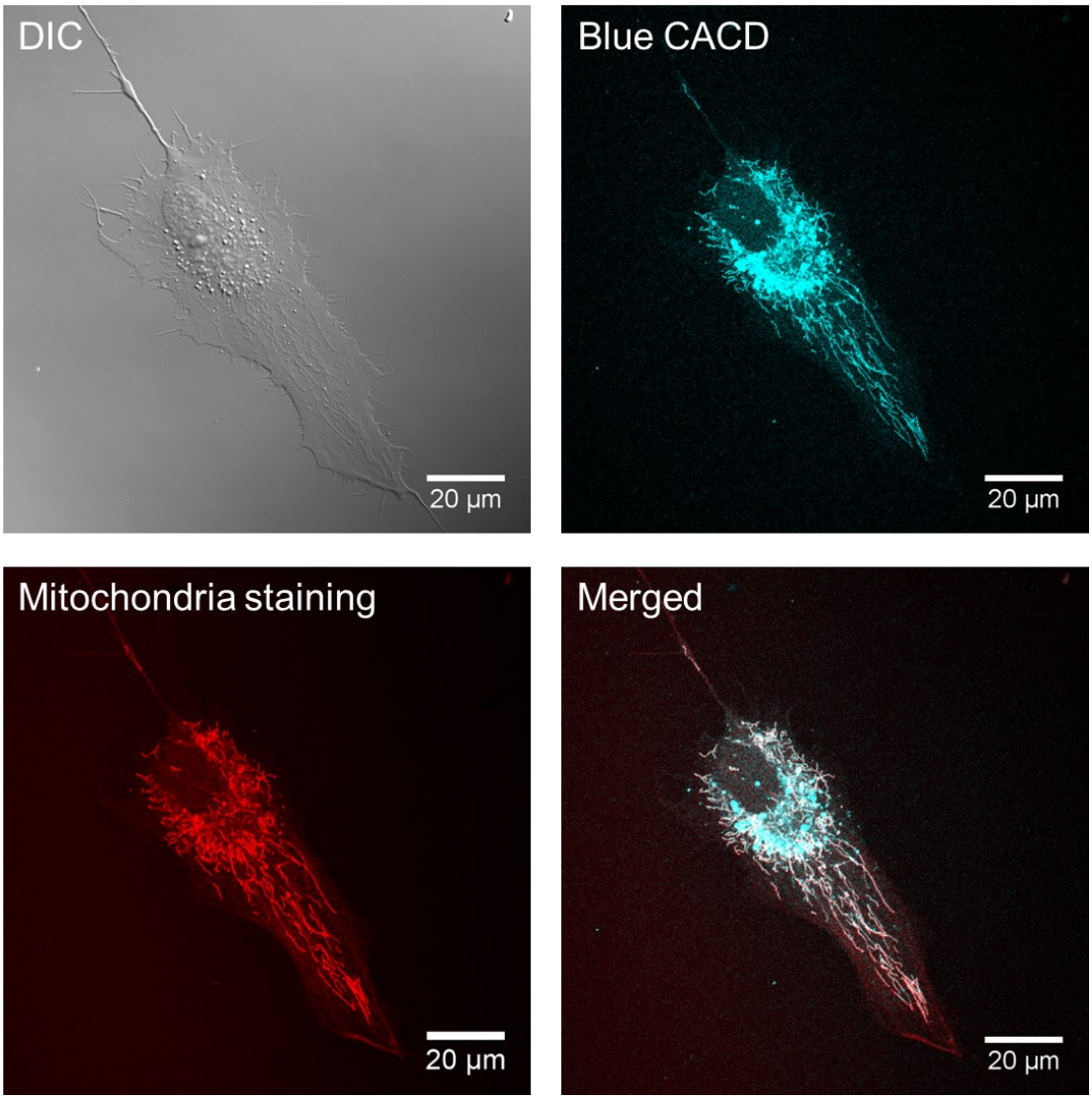

Figure S19. Some blue CDs localize with mitochondria upon uptake into trout gill epithelial cells.

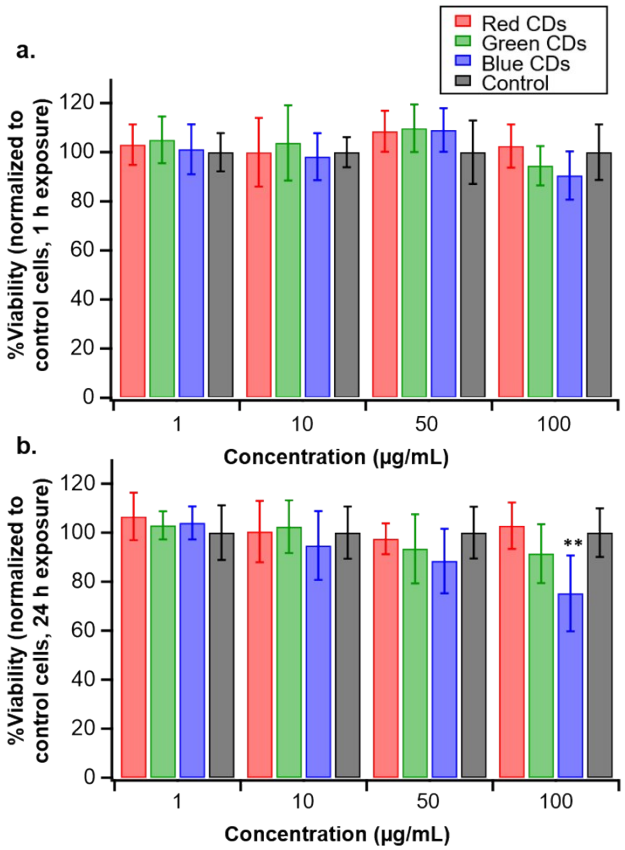

Figure S20. Impact of fractionated carbon dots on cell viability. (a) CD-B, CD-G, and CD-R caused no significant decrease in trout gill epithelial cell viability following 1 h exposure to 1, 10, 50, or 100 µg/mL of carbon dots. (b) CD-G and CD-R caused no significant decrease in cell viability following exposure for 24 h at all concentrations studied. CD-B did cause a significant decrease in cell viability following exposure to 100 µg/mL. **, $p < 0.01$.

Exchanges in REMD of citric acid + urea

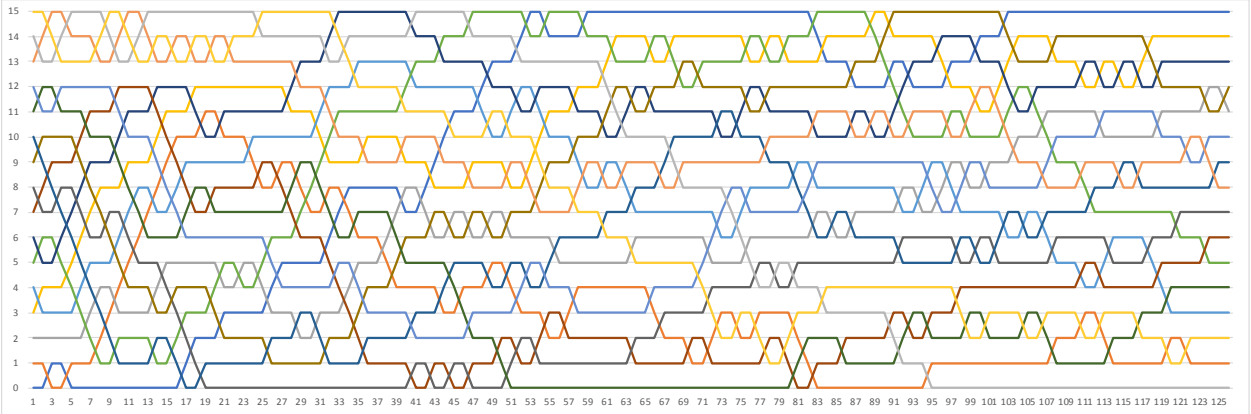

Figure S21. Plots of the exchanges among replicas in the REMD simulations for the polyamide decamer formed with citric acid and urea. The vertical axis corresponds to each replica (numbered 0 to 15) and the horizontal axis corresponds to an exchange attempt (exchange is attempted every 1 ps).

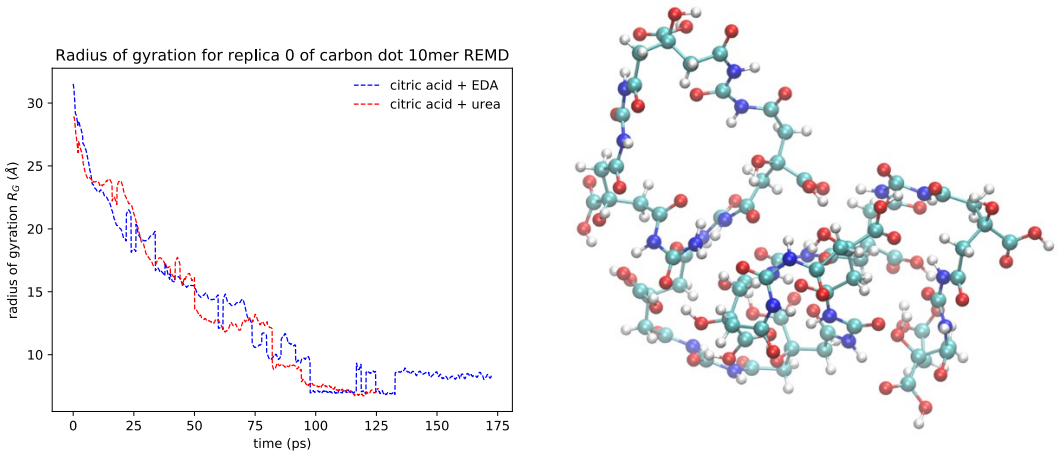

Figure S22. Radius of gyration for the replica at 300 K from REMD of the polyamide decamers from citric acid with urea (red). Also shown for comparison (blue) is a profile for the polyamide formed from citric acid with ethylene-diamine (EDA). A structural snapshot is shown on the right.

Table S1. XPS atomic percentage of C, N and O of raw products, blue, green and red CD fractions.

	C	N	O	N/C
Raw product	59.8%	17.2%	23.1%	0.29
B	41.2%	5.7%	47.6%	0.14
G	50.7%	7.5%	39.0%	0.15
R	48.5%	8.3%	40.5%	0.17

CHN elemental analysis of as-made CDs shows the formula is $C_{6.00}H_6N_{2.06}O_{5.26}$. It aligns with XPS elemental analysis, though not exactly the same. Other colored fractions were not done CHN elemental analysis due to lack of materials for the test.

Table S2. A list of solvents with dielectric constants, Kamlet Taft parameters (α, β, and π^*) and normalized solvent polarity E_T^N.[3-4]

	Dielectric constant	α	β	π^*	E_T^N
Acetone	20.7	0.08	0.48	0.71	0.355
DMF	36.7	0	0.69	0.88	0.386
DMSO	46.7	0	0.76	1	0.444
Ethanol	24.3	0.83	0.77	0.54	0.654
Methanol	32.6	0.93	0.62	0.6	0.762
Water	80	1.17	0.18	1.09	1

Table S3. Thermochemistry of small molecule chromophores based on B3LYP-D3/Def2TZVPP calculations following the reaction scheme shown in Figure S10.

		1	**2**	**3**
ΔH (kcal/mol) 298.15 K	Step1	-8.2	-0.02	-0.02
	Step2	29.8	20.9	27.5
	Overall	21.6	20.9	27.5
ΔG (kcal/mol) 298.15 K	Step1	-5.9	2.0	2.0
	Step2	9.2	-1.0	6.0
	Overall	3.3	1.0	8.0
ΔH (kcal/mol) 473.15 K	Step1	-8.1	0.2	0.2
	Step2	30.1	21.0	27.7
	Overall	22.0	21.2	27.9
ΔG (kcal/mol) 473.15 K	Step1	-4.6	3.2	3.2

	Step2	-3.0	-14.0	-6.7
	Overall	-7.6	-10.8	-3.5

Table S4. Thermochemistry of polyamide formation from citric acid and urea.

	Monomer	Monomer Dehydrated	Dimer Dehydrated
ΔH (kcal/mol) @298.15 K	-8.2	5.3	12.0
ΔG (kcal/mol) @298.15 K	-5.9	-4.5	3.1
ΔH (kcal/mol) @473.15 K	-8.1	5.6	12.6
ΔG (kcal/mol) @473.15 K	-4.6	-10.4	-2.3

a. For structures, see examples in Figure S13. Calculations were carried out at the B3LYP-D3/Def2TZVPP level of theory with harmonic approximations for the entropy calculations.

Table S5. TD-DFT results of Product **1** in Figure S10

Level of theory	Absorption			Emission		
	Excited State	λ (nm)	*f*	Excited State	λ (nm)	*f*
B3LYP/Def2TZVPP	1	355.2	0.0777	1	421.8	0.0671
	2	304.8	0.0073	2	335.3	0.0099
	3	272.4	0.0007	3	300.7	0.0000
ωB97XD/Def2TZVPP	1	330.1	0.1024	1	398.9	0.0871
	2	265.5	0.0038	2	284.1	0.0090
	3	250.4	0.0006	3	271.0	0.0003
ωB97XD/6-31+G(d,p)	1	330.0	0.1106	1	400.5	0.0929
	2	265.4	0.0044	2	286.2	0.0107
	3	251.1	0.0007	3	272.6	0.0002

Table S6. TD-DFT results of Product **2** in Figure S10

Level of theory	Absorption			Emission		
	Excited State	λ (nm)	*f*	Excited State	λ (nm)	*f*
B3LYP/Def2TZVPP	1	369.0	0.0001	1	923.6	0.0671
	2	342.2	0.0001	2	439.9	0.0001
	3	290.7	0.0295	3	419.0	0.0013
ωB97XD/6-31+G(d,p)	1	327.7	0.0000	1	562.2	0.0000
	2	301.0	0.0000	2	347.9	0.0001
	3	265.4	0.0152	3	332.6	0.0022

Table S7. TD-DFT results of Product **3** in Figure S10

Level of theory	Absorption			Emission		
	Excited State	λ (nm)	*f*	Excited State	λ (nm)	*f*
B3LYP/Def2TZVPP	1	375.7	0.0839	1	437.2	0.0716
	2	362.0	0.0001	2	387.5	0.0001
	3	281.2	0.0001	3	299.0	0.0000
ωB97XD/6-31+G(d,p)	1	339.2	0.1234	1	392.9	0.1104
	2	308.7	0.0003	2	328.9	0.0002
	3	253.5	0.0002	3	269.8	0.0001

Table S8. Emission (E), oscillator strength (*f*), and nature of the LC-TD-DFTB2 S2→S0 vertical relaxation for the polyamide dimer of citric acid and urea interacting with a small molecule chromophore and for the S1→S0 vertical relaxation calculated with TD-ωB97XD at the LC-TD-DFTB2 S2 optimized geometry.[a]

	LC-TD-DFTB2				TD-ωB97XD			
ID	E (eV)	E (nm)	f	Transition	E (eV)	E (nm)	f	Transition
0	3.528	351.43	0.142	HOMO-1 → LUMO	2.883	430.01	0.1162	HOMO → LUMO
1	3.647	339.96	0.112	HOMO → LUMO	2.990	414.70	0.0864	HOMO → LUMO
2	3.502	354.04	0.148	HOMO → LUMO	2.851	434.87	0.1184	HOMO → LUMO
3	3.630	341.55	0.155	HOMO-1 → LUMO	3.018	410.86	0.1182	HOMO → LUMO
4	3.703	334.82	0.146	HOMO → LUMO	3.094	400.78	0.1333	HOMO → LUMO
5	3.584	345.94	0.126	HOMO-2 → LUMO	3.059	405.33	0.1021	HOMO-1 → LUMO
6	3.666	338.20	0.103	HOMO-1 → LUMO	3.157	392.71	0.1091	HOMO → LUMO
7	4.225	293.45	0.158	HOMO-1 → LUMO	3.065	404.55	0.1099	HOMO → LUMO
8	3.339	371.32	0.127	HOMO-3	2.787	444.90	0.1059	HOMO →

				→ LUMO				LUMO
9	3.547	349.55	0.125	HOMO-3 → LUMO	2.949	420.43	0.1011	HOMO → LUMO

[a] For geometry ID 6, the S3→S0 vertical relaxation is reported.

Table S9. Absorption energy (Abs), emission energy (Em), and corresponding oscillator strengths (f) and nature of the S0→S1 transition for citric acid and urea polyamide dimer interacting with a small molecule chromophore. All geometries were optimized with (TD-) ωB97XD.

ID	Abs (eV)	Abs (nm)	*f*	Transition	Em (eV)	Em (nm)	*f*	Transition
0	3.713	333.95	0.135	HOMO → LUMO	2.955	419.53	0.089	HOMO → LUMO
1	3.644	340.23	0.111	HOMO → LUMO				
2	3.688	336.17	0.126	HOMO → LUMO	2.981	415.93	0.087	HOMO → LUMO
3	3.709	334.26	0.137	HOMO → LUMO	3.009	412.10	0.096	HOMO → LUMO
4	3.649	339.78	0.162	HOMO → LUMO	3.034	408.62	0.129	HOMO → LUMO

Table S10. Emission (E), oscillator strength (*f*), and nature of the LC-TD-DFTB2 bright vertical relaxation for the decamer of citric acid and urea interacting with the small molecule and for the S1→S0 vertical relaxation calculated with TD-ωB97XD/6-31+G(d) at the LC-TD-DFTB2 S2 optimized geometry.[a]

	LC-TD-DFTB2		TD-ωB97XD	
ID	E (nm)	f	E (nm)	f
0	350.8	0.094	422.6	0.076
1	335.5	0.110	398.2	0.095
2	364.6	0.111	464.9	0.071
3	356.2	0.125	430.3	0.097
4	341.1	0.130	410.6	0.104
5	338.6	0.110	400.7	0.100
6	359.8	0.115	433.0	0.082
7	357.7	0.078	419.1	0.068
8	336.1	0.121	---	---
9	345.8	0.114	414.7	0.106

Table S11. Thermochemistry of the pyrene-based model based on B3LYP-D3/Def2TZVPP calculations

$$P_0\text{: } C_6H_8O_7 \rightarrow \frac{9}{35}C_{18}H_{10}O_6 + \frac{48}{35}CO_2 + \frac{95}{35}H_2O$$

$$NP_X\text{: } C_6H_8O_7 + \frac{9}{28}CO(NH_2)_2 \rightarrow \frac{9}{28}C_{16}H_{10}O_6N_2 + \frac{33}{28}CO_2 + \frac{85}{28}H_2O$$

	P0	NP1	NP2	NP3	NP4
ΔH (kcal/mol)	-20.9	-0.8	2.5	4.0	4.2
ΔG (kcal/mol)	-53.4	-31.0	-27.8	-26.2	-26.1

Table S12. TD-DFT results of the pyrene-based model at the TD- ωB97XD/6-31+G(d) level of theory [a]

System		Absorption		Emission	
		λ (nm)	*f*	λ (nm)	*f*
P0(S0-S1)	Gas-phase	410.2	0.1576	455.8	0.1599
	Water	409.1	0.2013	474.3	0.3518
	Acetone	409.8	0.2051	473.0	0.3365
NP1(S0-S2)	Gas-phase	440.1	0.1171	525.2	0.0432
	Water	440.6	0.2587	532.9	0.3135
	Acetone	441.1	0.2643	531.6	0.2788
NP2(S0-S2)	Gas-phase	491.8	0.1098	614.1	0.0629
	Water	477.4	0.2123	596.7	0.272
	Acetone	478.9	0.2162	597.2	0.2493
NP3(S0-S2)	Gas-phase	488.2	0.1379	570.4	0.0547
	Water	493.6	0.2804	577.8	0.4727
	Acetone	494.0	0.286	575.3	0.4255
NP4(S0-S2)	Gas-phase	543.4	0.1568	692.9	0.1064
	Water	534.2	0.2474	706.0	0.3095
	Acetone	535.9	0.2521	704.8	0.2918

a. For water and acetone, PCM calculations were conducted with the TD-ωB97XD/6-31+G(d) level of theory.

Table S13. Absorption of NP4 calculated at the TD- ωB97XD/6-31+G(d) level of theory.

Absorption		
Excited State	λ (nm)	*f*
1	1092.0	0.0000
2	543.4	0.1570
3	459.8	0.0372
4	363.8	0.4184
5	298.5	0.0000
6	275.1	1.5608
7	265.2	0.0000
8	228.9	0.0000
9	217.7	0.3397
10	217.2	0.0002

Table S14. Absorption (Abs, in nm), emission (Em, in nm), oscillator strength (*f*), and nature of the S0→S1 transition for the polyamide dimer of citric acid and urea. All geometries are optimized with LC-TD-DFTB2.[a]

	LC-TD-DFTB2			ωB97XD			LC-TD-DFTB2		ωB97XD	
ID	Abs	*f*	Transition	Abs	*f*	Transition	Em	*f*	Em	*f*
0	242.31	0.0002	HOMO → LUMO	270.27	0.0001	HOMO → LUMO	395.51	0.0000	425.96	0.0000
1	235.41	0.0011	HOMO-1 → LUMO	252.12	0.0000	HOMO-1 → LUMO	434.55	0.0021	451.62	0.0016
2	240.30	0.0020	HOMO-1 → LUMO	256.73	0.0003	HOMO-1 → LUMO	407.85	0.0010	423.41	0.0008
3	237.54	0.0005	HOMO-3→ LUMO	260.09	0.0004	HOMO-5 → LUMO	478.44	0.0030	515.57	0.0020
4	242.12	0.0002	HOMO → LUMO	270.24	0.0001	HOMO → LUMO	394.49	0.0000	425.32	0.0000
5	233.11	0.0004	HOMO-1 → LUMO+1	265.26	0.0007	HOMO-1 → LUMO+2	496.40	0.0023	534.51	0.0015
6	234.95	0.0006	HOMO-2 → LUMO+1	260.82	0.0001	HOMO-3 → LUMO+1	474.55	0.0009	467.74	0.0017
7	244.19	0.0002	HOMO-1 → LUMO	267.31	0.0005	HOMO → LUMO	535.55	0.0000	449.19	0.0000
8	238.27	0.0006	HOMO-1 → LUMO	262.42	0.0000	HOMO → LUMO	446.97	0.0014	475.13	0.0013
9	240.59	0.0001	HOMO-1 → LUMO	270.87	0.0002	HOMO → LUMO	578.00	0.0013	461.39	0.0012

a. The basis set used in ωB97XD is 6-31+G(d).

Table S15. TD-DFT results of dehydrated amide: monomer [a]

Level of theory	Absorption			Emission		
	Excited State	λ (nm)	*f*	Excited State	λ (nm)	*f*
B3LYP/6-31+G(d,p)	1	334.6	0.0000	1	835.6	0.0000
	2	320.3	0.0062	2	691.0	0.0069
	3	312.7	0.0018	3	420.7	0.0002
ωB97XD/6-31+G(d,p)	1	271.0	0.0087	1	1602.2	0.0000
	2	246.8	0.0092	2	349.1	0.0001
	3	230.4	0.0780	3	328.5	0.0001
CAM-B3LYP/6-31+G(d,p)[b]	1	269.6	0.0087	1	1716.4	0.0000
	2	244.9	0.0088	2	348.2	0.0001
	3	230.3	0.0660	3	335.3	0.0001
CAM-B3LYP/6-31+G(d,p)[c]	1	283.3	0.0019	1	444.1	0.0000
	2	253.9	0.0024	2	409.3	0.0277
	3	242.3	0.0671	3	353.6	0.0000

a. For structures, see Figure S13.
b. Initial structures are taken from ωB97XD/6-31+G(d,p) optimizations.
c. Initial structures are taken from B3LYP/6-31+G(d,p) optimizations.

Table S16. TD-DFT results of the dehydrated amide: dimer

Level of theory	Absorption			Emission		
	Excited State	λ (nm)	*f*	Excited State	λ (nm)	*f*
ωB97XD/6-31+G(d,p)	1	273.6	0.0056	1	528.0	0.0031
	2	259.3	0.0125	2	341.6	0.0028
	3	250.0	0.0104	3	302.0	0.0051

Table S17. Oscillator strengths, *f*, of the first five singlet excitations for the polyamide dimer of citric acid and urea calculated at the ground state geometry optimized with LC-TD-DFTB2.

	0		1		2		3		4	
	LC-DFTB	ωB97XD	LC-DFTB	ωB97XD	LC-DFTB	ωB97XD	LC-DFTB	ωB97XD	LC-DFTB	ωB97XD
S1	0.000	0.000	0.001	0.000	0.002	0.000	0.001	0.000	0.000	0.000
S2	0.000	0.003	0.005	0.008	0.005	0.001	0.001	0.002	0.002	0.003
S3	0.003	0.001	0.000	0.001	0.000	0.009	0.003	0.005	0.003	0.002
S4	0.002	0.002	0.005	0.000	0.004	0.001	0.006	0.003	0.003	0.002
S5	0.003	0.001	0.001	0.002	0.001	0.002	0.010	0.002	0.003	0.001
	5		6		7		8		9	
	LC-DFTB	ωB97XD	LC-DFTB	ωB97XD	LC-DFTB	ωB97XD	LC-DFTB	ωB97XD	LC-DFTB	ωB97XD
S1	0.000	0.001	0.001	0.000	0.000	0.001	0.001	0.000	0.000	0.000
S2	0.001	0.002	0.000	0.001	0.001	0.002	0.000	0.003	0.002	0.003
S3	0.001	0.002	0.001	0.002	0.000	0.002	0.003	0.001	0.001	0.001
S4	0.002	0.002	0.004	0.004	0.000	0.003	0.005	0.001	0.008	0.001
S5	0.011	0.003	0.008	0.001	0.003	0.001	0.001	0.002	0.002	0.002

Table S18. Excitation energy (in eV) of the S0→S1 for the polyamide formed from citric acid and ethylene diamine studied in Ref. 1.[a]

Structure	B3LYP	ωB97XD	CAM-B3LYP	DFTB3	DFTB2	LC-DFTB2
Dimer (one chain)	5.182	5.690	5.670	3.925	5.780	5.996
Dimer (two chain) intramolecular HB	4.878	5.635	5.620	3.538	5.351	5.957
Dimer (two chain) intermolecular HB	5.144	5.528	5.514	4.198	5.945	5.905
Octamer	4.619	5.394	5.397	3.371	4.643	5.436
Decamer	4.647	5.384	5.384	3.447	4.742	5.390

[a] For DFT methods, the basis set used was 6-31G(d). For DFTB3, the 3OB parameter set was used. For DFTB2, the OB2/base parameters set was used. The DFTB parameters were obtained from www.dftb.org. As shown in Fig. S8, the S1 excitation at the B3LYP level is charge transfer in nature, while the nature of excitation is local when range-separation functionals are used in either TD-DFT or TD-DFTB calculations. Overall, the results of TD-DFTB are in good agreement with ωB97XD and CAM-B3LYP once a range-separation functional is used (LC-DFTB2).

Reference

1. Bhattacharya, D.; Mishra, M. K.; De, G., Carbon Dots from a Single Source Exhibiting Tunable Luminescent Colors through the Modification of Surface Functional Groups in ORMOSIL Films. *J. Phys. Chem. C* **2017,** *121* (50), 28106-28116.

2. Liu, W.; Li, C.; Ren, Y.; Sun, X.; Pan, W.; Li, Y.; Wang, J.; Wang, W., Carbon dots: surface engineering and applications. *J. Mater. Chem. B* **2016,** *4* (35), 5772-5788.

3. Jones, S. S.; Sahatiya, P.; Badhulika, S., One step, high yield synthesis of amphiphilic carbon quantum dots derived from chia seeds: a solvatochromic study. *New J. Chem.* **2017,** *41* (21), 13130-13139.

4. Reichardt, C., Solvatochromic dyes as solvent polarity indicators. *Chem. Rev.* **1994,** *94* (8), 2319-2358.